CrossMark

ORIGINAL PAPER

Breather-to-soliton and rogue wave-to-soliton transitions in a resonant erbium-doped fiber system with higher-order effects

Lei Wang · Shen Li · Feng-Hua Qi

Abstract Under investigation in this paper is the higher-order nonlinear Schrödinger and Maxwell–Bloch system which describes the wave propagation in an erbium-doped nonlinear fiber with higher-order effects including the fourth-order dispersion and quintic non-Kerr nonlinearity. The breather and rogue wave (RW) solutions are shown that they can be converted into various soliton solutions including the multi-peak soliton, periodic wave, antidark soliton, M-shaped soliton, and W-shaped soliton. In addition, under different values of higher-order effect, the locus of the eigenvalues on the complex plane which converts breathers or RWs into solitons is calculated.

L. Wang (✉)
Department of Mathematics and Physics, North China Electric Power University, Beijing 102206, People's Republic of China
e-mail: wanglei2239@126.com

S. Li
School of Electrical and Electronic Engineering, North China Electric Power University, Beijing 102206, People's Republic of China

F.-H. Qi
School of Information, Beijing Wuzi University, Beijing 101149, People's Republic of China

1 Introduction

Optical solitons have attracted considerable interest of scientists around the world during the past decades [1]. In optical fibers, there are two different types of solitons. One is described by the nonlinear Schrödinger (NLS) equation [2,3], the mechanism of which is based on the balance between the second-order dispersion and Kerr nonlinearity. This type of soliton is called the NLS soliton. The other type of lossless pulse propagation is the self-induced transparency (SIT) soliton in the two-level resonance medium, the dynamic response of which is governed by the Maxwell–Bloch (MB) system [4,5]. When erbium is doped with the core of the optical fibers, the NLS soliton can exist with the SIT soliton. The propagation of such pulse can be modeled by the NLS–MB system [6–10]. However, in an optical-fiber transmission system, one always needs to increase the intensity of the incident light field to produce ultrashort optical pulses [11–17]. Thus, such higher-order effects as the higher-order dispersion, higher-order nonlinearity, self-steepening, and self-frequency shift should be included [11–17].

In this paper, we will work on the higher-order NLS–MB system as follows [18–22],

$$E_z = \mathrm{i}\,(E_{tt} + 2\,|E|^2\,E) + \mathrm{i}\,\tau\,(E_{tttt} + 8\,|E|^2\,E_{tt}$$
$$+ 2\,E^2\,E_{tt}^* + 6\,E^*\,E_t^2 + 4\,|E_t|^2\,E$$
$$+ 6\,|E|^4\,E) + 2\,p,$$

$$p_t = 2\mathrm{i}\,\omega p + 2\,E\eta,$$
$$\eta_t = -(Ep^* + E^*p), \tag{1.1}$$

where the subscripts z, t are partial derivatives with respect to the distance and time, and the asterisk symbol stands for the complex conjugate. E denotes the normalized slowly varying amplitude of the complex field envelope, $p = v_1 v_2^*$ represents as the polarization, and $\eta = |v_1|^2 - |v_2|^2$ means the population inversion with v_1 and v_2 being the wave functions of the two energy levels of the resonant atoms, ω is the frequency, and τ is a small dimensionless real parameter.

Various solutions of System (1.1) have been discussed. For example, based on the Lax pair and Darboux transformation (DT), the multi-soliton solutions of System (1.1) have been presented in Ref. [18]. The breather, rogue wave (RW), and hybrid solutions of System (1.1) have been obtained by means of the generalized DT in Refs. [19–22]. Solitons, breathers, and RWs are different types of nonlinear localized waves and are central objects in diverse nonlinear physical systems [23–37]. The hybrid solutions, which are expressed in the form of the mixed rational–exponential functions, describe the nonlinear superposition of the RW and breather [38]. Recently, Liu et al. [39] have shown that the breathers can be converted into different types of nonlinear waves in the coupled NLS–MB system, including the multi-peak soliton, periodic wave, antidark soliton, and W-shaped soliton. These conversions occur under a special condition in which the soliton and a periodic wave in the breather have the same velocity [39]. In addition, the similar transitions have also been reported in some higher-order nonlinear equation of evolutions. Akhmediev et al. have found that the breather solutions of the Hirota [40] equation and fifth-order NLS [41] equation can be converted into soliton solutions on the constant background, which does not exist in the standard NLS equation. Liu et al. have revealed that the transition between the soliton and RW occurs as a result of the attenuation of MI growth rate to vanishing in the zero-frequency perturbation region [42,43].

It is natural to ask: Can the transition between the breather (or RW) and soliton occur in the higher-order coupled system, e.g., System (1.1)? In this paper, we show that System (1.1) does have such transition when the eigenvalues are located at the special locus on the complex plane. Further, we demonstrate that the breather can be converted into the multi-peak soliton,

periodic wave, antidark soliton, and M-shaped soliton while the RW can be transformed into the W-shaped soliton.

The outline of this paper will be as follows: The breather-to-soliton conversion and several types of transformed nonlinear waves will be studied in Sect. 2. The RW-to-soliton conversion will be discussed in Sect. 3. Finally, our conclusions will be addressed in Sect. 4.

2 Breather-to-soliton conversions

In this section, we present different types of nonlinear wave solutions on constant background for System (1.1). We omit the discussions of the components p and η because the types of them have the similar characteristics as E. Based on the lax pair and DT [18–22] of System (1.1), the first-order symmetric breather solution reads as

$$E_B^{[1]} = d\left(1 + 8\,n\,\frac{G_B^{[1]} + \mathrm{i}\,H_B^{[1]}}{D_B^{[1]}}\right)\mathrm{e}^{\mathrm{i}\,\rho},$$

$$p_B^{[1]} = \frac{1}{2}\left(\left(E_B^{[1]}\right)_z - \mathrm{i}\left(\left(E_B^{[1]}\right)_{tt} + 2\,|E_B^{[1]}|^2\,E_B^{[1]}\right)\right.$$
$$- \mathrm{i}\,\tau\left(\left(E_B^{[1]}\right)_{tttt} + 8\left|E_B^{[1]}\right|^2\left(E_B^{[1]}\right)_{tt}\right.$$
$$+ 2\left(E_B^{[1]}\right)^2\left(E_B^{[1]}\right)_{tt}^* + 6\left(E_B^{[1]}\right)^*\left(E_B^{[1]}\right)_t^2$$
$$+ 4\left|\left(E_B^{[1]}\right)_t\right|^2 E_B^{[1]} + 6\,|E_B^{[1]}|^4\,E_B^{[1]}\Big)\Big),$$

$$\eta_B^{[1]} = \frac{-2\,\mathrm{i}\,\omega\left(p_B^{[1]}\right)^{[1]} + \left(p_B^{[1]}\right)_t^{[1]}}{2\,E_B^{[1]}}. \tag{2.1}$$

where

$$G_B^{[1]} = 2\,k_1\,k_2\,n\,\cos(t\,h_R + z\,\varpi_B)$$
$$+ 2\,n\,\cosh(t\,h_I + z\,\varpi_A)$$
$$- k_1\,k_2\,h_R\,\sin(t\,h_R + z\,\varpi_B)$$
$$+ h_I\,\sinh(t\,h_I + z\,\varpi_A),$$

$$H_B^{[1]} = k_1\,k_2\,(b + 2\,m)\,\cos(t\,h_R + z\,\varpi_B)$$
$$+ (b + 2\,m)\,\cosh(t\,h_I + z\,\varpi_A)$$
$$+ k_1\,k_2\,h_I\,\sin(t\,h_R + z\,\varpi_B)$$
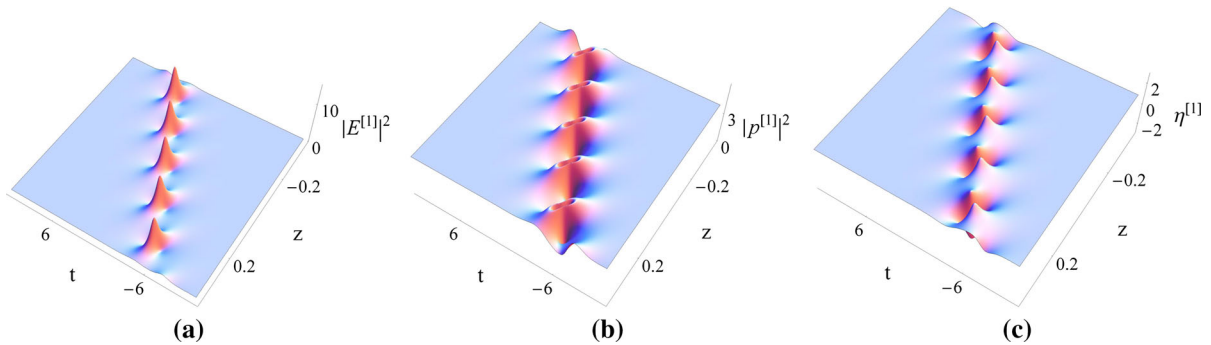$$+ h_R\,\sinh(t\,h_I + z\,\varpi_A),$$

Fig. 1 First-order breather solution of the NLS–MB system (E, p, η) with $d = 1, b = 2, k_1 = -k_2 = 1, \omega = \frac{1}{2}, \tau = \frac{1}{2}$ and $\lambda_1 = \lambda_2^* = -1.2 + i$

$$D_B^{[1]} = k_1 k_2 (|h|^2 - \chi) \cos(t h_R + z \varpi_B)$$
$$- (|h|^2 + \chi) \cosh(t h_I + z \varpi_A)$$
$$- k_1 k_2 \Gamma_A \sin(t h_R + z \varpi_B)$$
$$- \Gamma_B \sinh(t h_I + z \varpi_A),$$

with

$$\rho = a z + b t, \quad \lambda = m + i n,$$
$$a = (b^4 - 12 b^2 d^2 + 6 d^4) \tau - (b^2 - 2 d^2)$$
$$+ \frac{4}{2 \omega - b},$$
$$\chi = 4 m^2 + 4 n^2 + 4 m b + b^2 + 4 d^2,$$
$$\Gamma_A = 2 b h_I + 4 m h_I - 4 n h_R,$$
$$\Gamma_B = 2 b h_R + 4 m h_R + 4 n h_I,$$
$$\varpi_A = 2(\kappa_R h_I + \kappa_I h_R),$$
$$\varpi_B = 2(\kappa_R h_R - \kappa_I h_I),$$
$$\kappa = \frac{1}{2}(-b + 2\lambda + (b^3 - 6 b d^2 + (4 d^2 - 2 b^2)\lambda$$
$$+ 4 b \lambda^2 - 8 \lambda^3) \tau) - \frac{1}{(b - 2\omega)(\lambda + \omega)}$$
$$= \kappa_R + i \kappa_I,$$
$$h = 2 \sqrt{d^2 + \left(\lambda + \frac{b}{2}\right)^2} = h_R + i h_I.$$

Solution (2.1) includes the hyperbolic functions $\sinh$ $(t h_I + z \varpi_A)$ (or $\cosh(t h_I + z \varpi_A)$) and the trigonometric functions $\sin(t h_R + z \varpi_B)$ (or $\cos(t h_R + z \varpi_B)$), where $\kappa_R + \frac{\kappa_I h_R}{h_I}$ and $\kappa_R - \frac{\kappa_I h_I}{h_R}$ are the corresponding velocities. In this case, the hyperbolic functions and trigonometric functions, respectively, characterize the localization and the periodicity of the transverse distribution t of those waves. The nonlinear structure described by Solution (2.1) can be seen as a nonlinear combination of a soliton with the velocity $\kappa_R + \frac{\kappa_I h_R}{h_I}$

and a periodic wave with the velocity $\kappa_R - \frac{\kappa_I h_I}{h_R}$. Next, we will display various nonlinear wave structures depending on the values of velocity difference, namely $\frac{\kappa_I (h_R^2 + h_I^2)}{h_R h_I}$.

If the velocity difference is not equal to zero, i.e., $\kappa_I (\frac{h_R^2 + h_I^2}{h_R h_I}) \neq 0$ (or $k_I \neq 0$), Solution (2.1) characterizes the localized waves with breathing behavior on a plane-wave background (i.e., the breathers and RWs). Further, if $m = -\frac{b}{2}$, we have the Akhmediev breathers with $|n| < |d|$, the Kuznetsov–Ma solitons with $|n| > |d|$, and the Peregrine soliton with $|n| = |d|$. Such solutions have been derived in Refs. [19–22] (also see Fig. 1).

Instead, if $\kappa_I = 0$, the wave described by Solution (2.1) is composed of a soliton and a periodic wave, where each has the same velocity κ_R. It should be noted that the case $\kappa_I = 0$ is equivalent to

$$\frac{\varpi_A}{h_I} = \frac{\varpi_B}{h_R}, \tag{2.2}$$

i.e.,

$$\tau = \frac{\Theta_1}{\Theta_2}, \tag{2.3}$$

where

$$\Theta_1 = (b - 2\omega)\left((m + \omega)^2 + n^2\right) + 1,$$
$$\Theta_2 = (b - 2\omega)\left((m + \omega)^2 + n^2\right)$$
$$\left(b^2 - 4bm - 2(d^2 - 6m^2 + 2n^2)\right).$$

Equation (2.2) [i.e., Eq. (2.3)] implies the extrema of trigonometric and hyperbolic functions in Solution (2.1) is located along the same straight lines in the
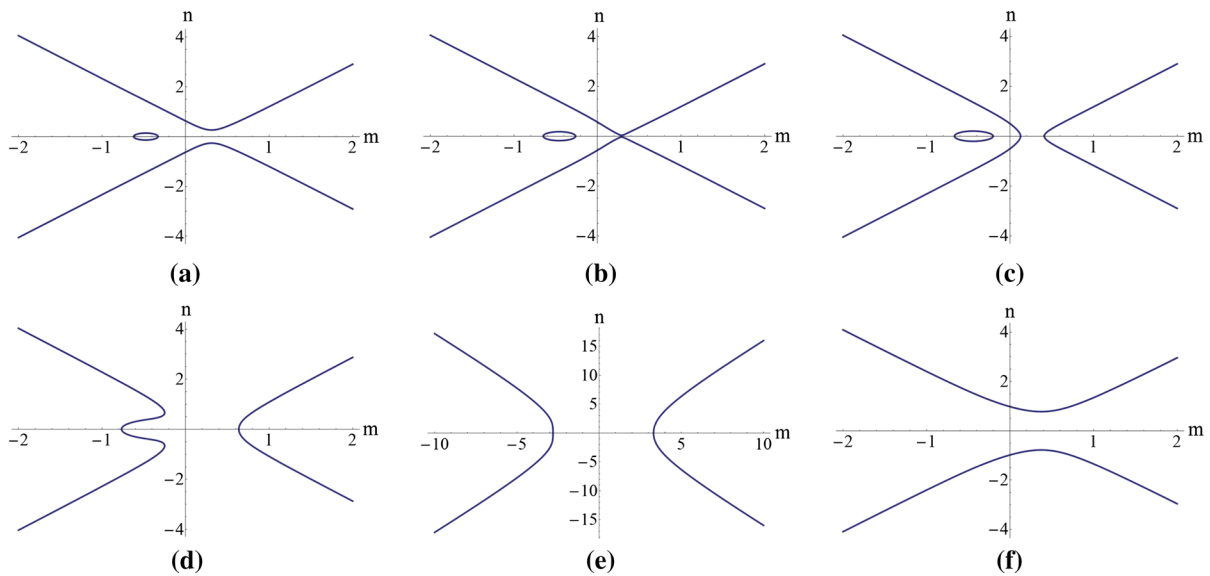
Fig. 2 Solutions of Eq. (2.3) on a complex plane of $\lambda_1 = m + n\,\mathrm{i}$. $d = 1$, $b = 2$, $\omega = \frac{1}{2}$. **a** $\tau = 6$, **b** $\tau = 3.8$, **c** $\tau = 3$, **d** $\tau = 1$, **e** $\tau = 0.01$, **f** $\tau = -1$

(z, t)-plane, which leads to the transformation of the breather into a continuous soliton. Choosing different values of τ in Eq. (2.3), we display the locus of the real and imaginary parts of the eigenvalues on the complex plane in Fig. 2. It is found that the higher-order effect τ can alter the shape of the locus. By decreasing the value of τ, we find that the quantity of branches of the locus is reduced from three to two.

When the six parameters m, n, ω, τ, b, and d satisfy Eq. (2.3), Expressions (2.1) describe the soliton on constant background, as shown in Fig. 3. This type of multi-peak structure is because of the mixture of a soliton and a periodic wave. The similar multi-peak structures have been observed analytically in the NLS–MB equations [39] and numerically in the AC-driven damped NLS system [44,45]. Further, to exhibit the effect of the real part (m) of the eigenvalue on the peak number, we plot Fig. 4 where the soliton has significantly less peaks than the one in Fig. 3. On the other hand, due to the different choices of the value of the eigenvalue, Fig. 5 shows the soliton with two main peaks, which is referred to as the M-shaped soliton in this paper. Note that the multi-peak solitons in Figs. 3, 4, and 5 are the localized structures along the t axis. However, changing the values of the real and imaginary parts of eigenvalue, we display another type of solution that shows a type of nonlocal structure, i.e., the periodic wave (see Fig. 6). Therefore, it is concluded

that the structure (peak number and localization) of the multi-peak soliton can be controlled by the real and imaginary parts of eigenvalue, namely m and n.

In order to better understand this multi-peak structure of System (1.1), we will extract separately the soliton and periodic wave from the mixed solution (2.1). Specifically, the soliton exists in isolation when h_R vanishes, while the periodic wave independently exists when h_I vanishes. Correspondingly, the analytic expressions read, for the antidark soliton,

$$E_S^{[1]} = d\left(1 + 8n\,\frac{G_S^{[1]} + \mathrm{i}\,H_S^{[1]}}{D_S^{[1]}}\right)\mathrm{e}^{\mathrm{i}\rho} \qquad (2.4)$$

with

$$
\begin{aligned}
G_S^{[1]} &= 2n\,\cos(2z\kappa_I h_I) + 2n\,\cosh(t\,h_I + 2z\kappa_R h_I) \\
&\quad + h_I\,\sinh(t\,h_I + 2z\kappa_R h_I), \\
H_S^{[1]} &= (b+2m)\,\cos(2z\kappa_I h_I) + (b+2m)\,\cosh(t\,h_I \\
&\quad + 2z\kappa_R h_I) - h_I\,\sin(2z\kappa_I h_I), \\
D_S^{[1]} &= \left(h_I^2 - \chi\right)\cos(2z\kappa_I h_I) - \left(h_I^2 + \chi\right)\cosh(t\,h_I \\
&\quad + 2z\kappa_R h_I) + (2b\,h_I + 4m\,h_I)\,\sin(2z\kappa_I h_I) \\
&\quad - 4n\,h_I\,\sinh(t\,h_I + 2z\kappa_R h_I),
\end{aligned}
$$

and for the periodic wave,

$$E_P^{[1]} = d\left(1 + 8n\,\frac{G_P^{[1]} + \mathrm{i}\,H_P^{[1]}}{D_P^{[1]}}\right)\mathrm{e}^{\mathrm{i}\rho} \qquad (2.5)$$
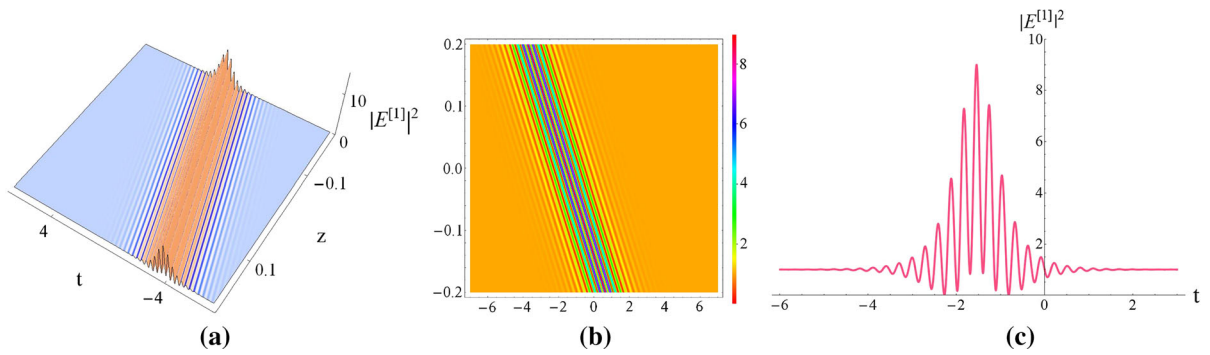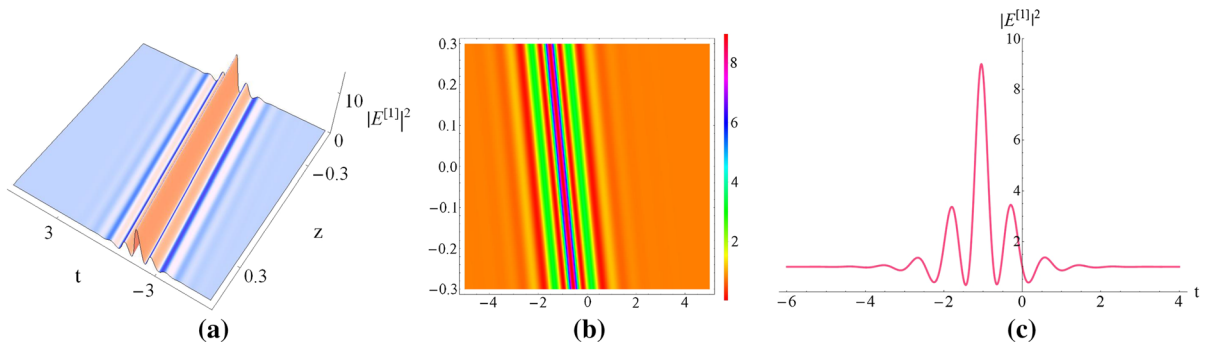
Fig. 3 A breather transformed into a multi-peak soliton with $d = 1, b = 2, k_1 = -k_2 = 1, \omega = \frac{1}{2}$ and $\lambda_1 = \lambda_2^* = 9.6 + \mathrm{i}$. **b** is the contour plot of **a**. **c** is the cross-sectional view of (**a**) at $z = 0$

Fig. 4 A breather transformed into a multi-peak soliton with $d = 1, b = 2, k_1 = -k_2 = 1, \omega = \frac{1}{2}$ and $\lambda_1 = \lambda_2^* = 2.5 + \mathrm{i}$. **b** is the contour plot of **a**. **c** is the cross-sectional view of (**a**) at $z = 0$
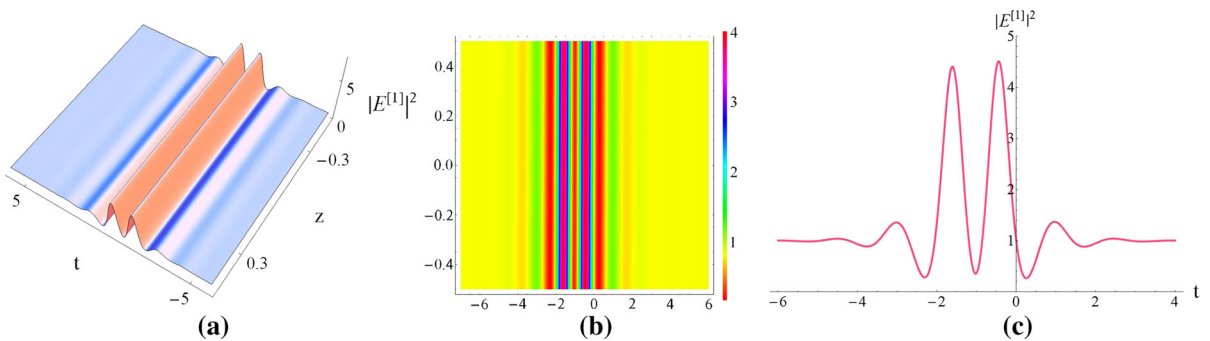

Fig. 5 A breather transformed into a M-shaped soliton with $d = 1, b = 2, k_1 = -k_2 = 1, \omega = \frac{1}{2}$ and $\lambda_1 = \lambda_2^* = 0.9 + 0.8\,\mathrm{i}$. **b** is the contour plot of **a**. **c** is the cross-sectional view of (**a**) at $z = 0$

with
$$G_P^{[1]} = -2n\,\cos(t\,h_R + 2\,z\,\kappa_R\,h_R)$$
$$+2n\,\cosh(2\,z\,\kappa_I\,h_R)$$
$$+h_R\,\sin(t\,h_R + 2\,z\,\kappa_R\,h_R),$$
$$H_P^{[1]} = -(b + 2m)\,\cos(t\,h_R + 2\,z\,\kappa_R\,h_R)$$
$$+(b + 2m)\,\cosh(2\,z\,\kappa_I\,h_R)$$
$$+h_R\,\sinh(2\,z\,\kappa_I\,h_R),$$

$$D_P^{[1]} = -(h_R^2 - \chi)\,\cos(t\,h_R + 2\,z\,\kappa_R\,h_R)$$
$$- (h_R^2 + \chi)\,\cosh(2\,z\,\kappa_I\,h_R)$$
$$-4n\,h_R\,\sin(t\,h_R + 2\,z\,\kappa_R\,h_R)$$
$$-(2\,b\,h_R + 4\,m\,h_R)\,\sinh(2\,z\,\kappa_I\,h_R).$$

Figure 7 describes a soliton on the constant background, which propagates along t direction. This kind of soliton is called the antidark soliton firstly reported
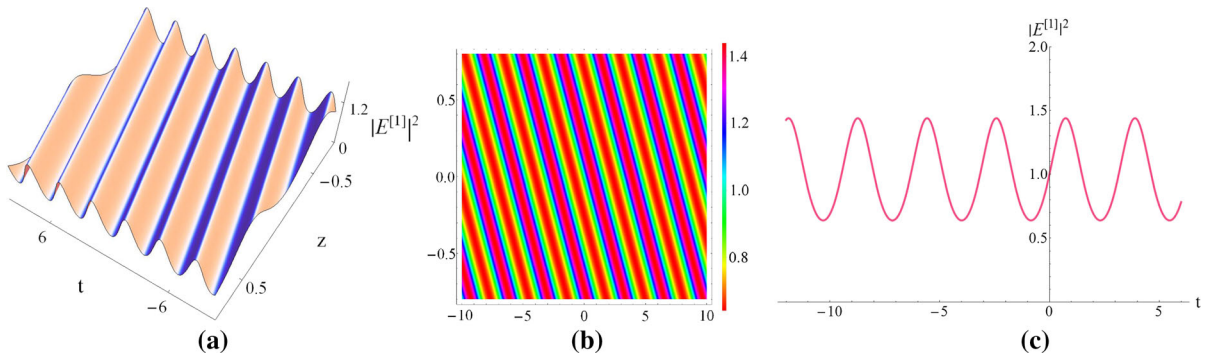
Fig. 6 A breather transformed into a multi-peak soliton (equal-amplitude) with $d = 1, b = 2, k_1 = -k_2 = 1, \omega = \frac{1}{2}$ and $\lambda_1 = \lambda_2^* = -1 - 0.1\,\mathrm{i}$. **b** is the contour plot of **a**. **c** is the cross-sectional view of (**a**) at $z = 0$
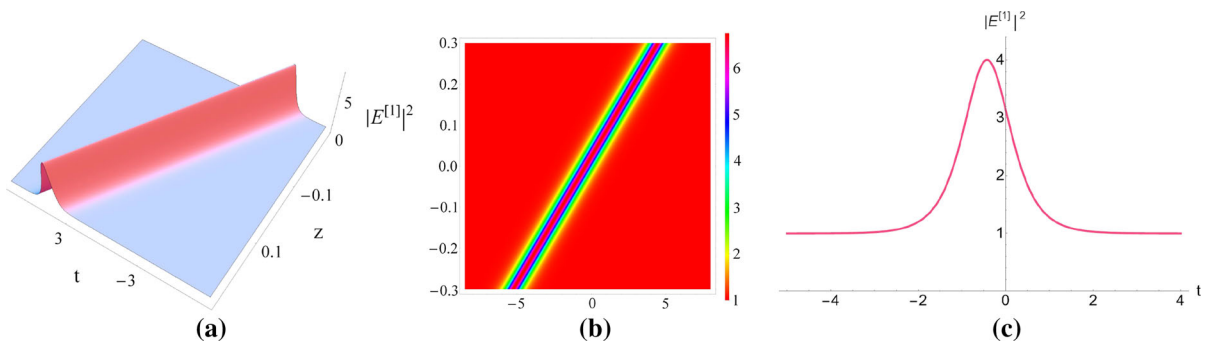

Fig. 7 A breather transformed into an antidark soliton with $d = 1, b = 2, k_1 = k_2 = 1, \omega = \frac{1}{2}$ and $\lambda_1 = \lambda_2^* = -\frac{1}{2} b + 1.5\,\mathrm{i}$. **b** is the contour plot of **a**. **c** is the cross-sectional view of (**a**) at $z = 0$
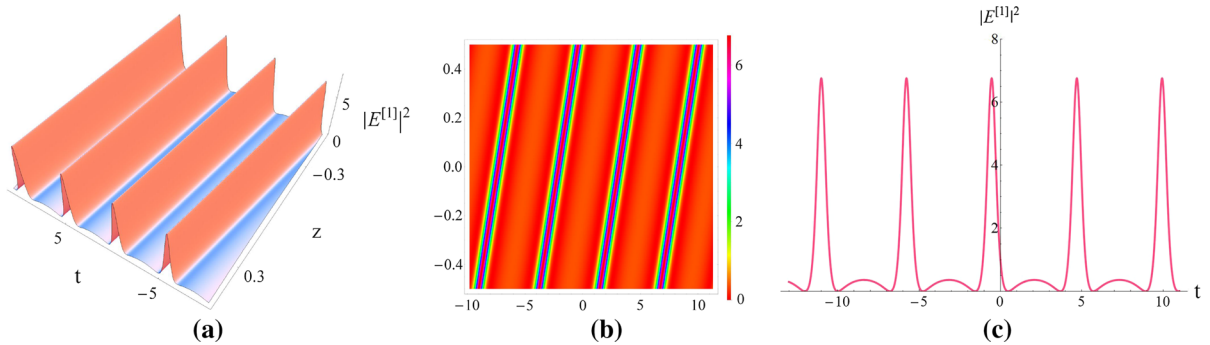

Fig. 8 A breather transformed into period wave with $d = 1, b = 2, k_1 = -k_2 = 1, \omega = \frac{1}{2}$ and $\lambda_1 = \lambda_2^* = -\frac{1}{2} b + 0.8\,\mathrm{i}$. **b** is the contour plot of **a**. **c** is the cross-sectional view of (**a**) at $z = 0$

in the scalar NLS system with the third-order dispersion [46,47]. Futher, as d is approaching to zero, this soliton will turn into a standard bright soliton. Figure 8 is plotted for the periodic waves propagating in t direction with the period $P = \frac{\pi}{h_R}$.

3 RW-to-soliton conversion

In this section, we investigate the transition of first-order localized wave $|E_1(t, z)|^2$ from the RW to the W-shaped traveling wave. Taking $\lambda \to -\frac{b}{2} + \mathrm{i} d$ in Solution (2.1), we obtain the first-order RW which is

Fig. 9 First-order asymmetric RW solution with $d = 1, b = 2, k_1 = -k_2 = 1, \omega = \frac{1}{2}, \tau = \frac{1}{2}$ and $\lambda_1 = \lambda_2^* = -\frac{1}{2} b + \mathrm{i} d$
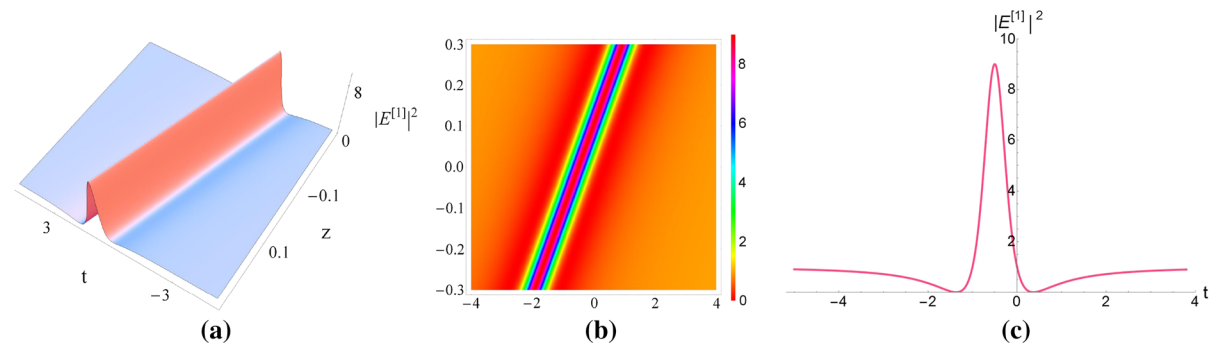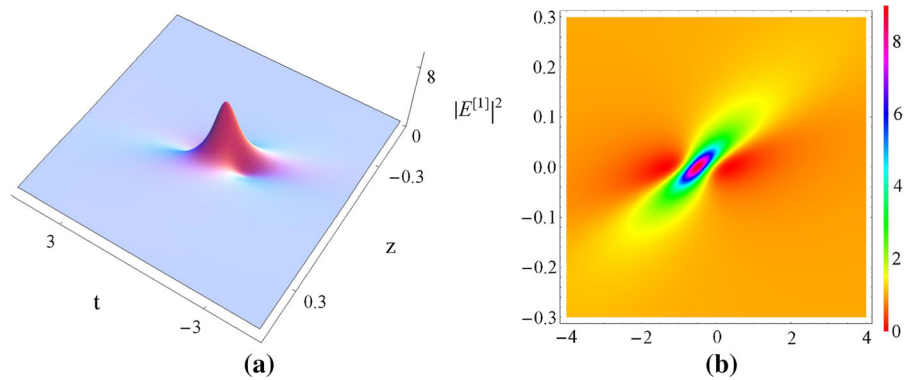

(a)

(b)

(a)

(b)

(c)

Fig. 10 An asymmetric RW transformed into a W-shaped soliton with $d = 1, b = 0, k_1 = -k_2 = 1, \omega = \frac{1}{2}$ and $\lambda_0 = -\frac{1}{2} b + \mathrm{i} d$. **b** is the contour plot of **a**. **c** is the cross-sectional view of (**a**) at $z = 0$

asymmetric with respect to z-axis in Fig. 9. Further, to convert the asymmetric RW into a soliton, the parameters ω, τ and b have to satisfy Eq. (2.3). Unlike the cases in Sect. 3, such transition is only controlled by three free parameters due to the fixed values of the real ($m = -\frac{b}{2}$) and imaginary ($n = d$) parts of the eigenvalue. In addition, Expression (3.1) has the forms of rational functions. Note that the rational solutions of the modified NLS equation have been found that they can describe various soliton states including a paired bright–bright soliton, single soliton, a paired bright-gray soliton, a paired bright-black soliton, which is induced by self-steepening and self-phase modulation through tuning the values of the corresponding free parameters [48,49]. Hereby, we display that the rational solution of System (1.1) characterizes the W-shaped soliton which is shown in Fig. 10. Different from the wave in Figs. 3 and 4, the soliton in Fig. 10 has only one (two), infinitely stretched, peak (valleys) without oscillatory tails. It is worth noting that the W-shaped soliton can be also converted by the periodic wave in Fig. 8 when the period is infinite ($h_R \to 0$). In other words,

there are two orders to obtain the W-shaped soliton: one is the breather$\to$ RW $\to$ W-shaped soliton and the other is the breather$\to$periodic wave$\to$W-shaped soliton.

$$E_W^{[1]} = d \left(1 - \frac{\Upsilon_1}{\Upsilon_2} \right) \mathrm{e}^{\Upsilon_3} \qquad (3.1)$$

with

$$\begin{aligned}
\Upsilon_1 = {} & 4d(-8\omega^3(4b^3 dz + 6bd^3 z - 3(b - d) \\
& \times (b + d)(dt + 1)) + 12b\omega^2(4b^3 dz + 6bd^3 z \\
& - 3(b - d)(b + d)(dt + 1)) - 3(b^5 + 3b^3 d^2 \\
& - 4bd^4)(dt + 1) + 2bdz((11b^3 + 30)d^2 \\
& + 2b^2(b^3 - 5) + 12bd^4) - 2\omega(2dz((17b^3 + 6)d^2 \\
& + 6b^2(b^3 - 1) + 12bd^4) - 3(3b^4 + b^2 d^2 \\
& - 4d^4)(dt + 1)))(4b^6 z - 3b^5(t + 8\omega z) \\
& + 2b^4(11d^2 z + 3\omega(3t + 8\omega z)) \\
& - b^3(d^2(9t + 68\omega z) + 4\omega^2(9t + 8\omega z) + 20z) \\
& + 6b^2(4d^4 z + d^2\omega(t + 12\omega z) + 4\omega(t\omega^2 + z)) \\
& + 12bd^2(d^2(t - 4\omega z) + 3t\omega^2 - 4\omega^3 z + 5z) \\
& - 24d^2\omega(t(d^2 + \omega^2) + z)),
\end{aligned}$$

$$\Upsilon_2 = 32d^2z^2b^{12} - 24dzb^{11} - 48d^2tzb^{11}$$
$$+ 18d^2t^2b^{10} + 352d^4z^2b^{10} + 18dtb^{10} + 9b^{10}$$
$$- 320d^2z^2b^9 - 204d^3zb^9$$
$$- 408d^4tzb^9 + 54d^2b^8 + 108d^4t^2b^8 + 1352d^6z^2b^8$$
$$+ 108d^3tb^8 + 120dzb^8 + 240d^2tzb^8 - 800d^4z^2b^7$$
$$- 444d^5zb^7 - 888d^6tzb^7 + 9d^4b^6 + 18d^6t^2b^6$$
$$+ 2112d^8z^2b^6 + 800d^2z^2b^6$$
$$+ 18d^5tb^6 + 3360d^6z^2b^5 + 96d^7zb^5$$
$$+ 192d^8tzb^5 - 216d^6b^4 - 432d^8t^2b^4 + 1152d^{10}z^2b^4$$
$$- 4800d^4z^2b^4 - 432d^7tb^4 - 1560d^5zb^4 - 3120d^6tzb^4$$
$$+ 5760d^8z^2b^3 + 576d^9zb^3 + 1152d^{10}tzb^3 + 144d^8b^2$$
$$+ 288d^{10}t^2b^2 + 7200d^6z^2b^2 + 288d^9tb^2$$
$$+ 1440d^7zb^2 + 2880d^8tzb^2 - 192(9(b-d)^2$$
$$(2dt(dt+1)+1)(b+d)^2 + 8b^2d^2(2b^2+3d^2)^2z^2$$
$$- 12d(2b^5 + d^2b^3 - 3d^4b)(2dt+1)z)\omega^5b$$
$$- 32(9(b-d)^2(5b^2+8d^2)(2dt(dt+1)+1)$$
$$(b+d)^2 - 12(b-d)d(24bd^4 + (31b^3 + 12)d^2$$
$$+ b^2(10b^3 - 7))(2dt+1)z(b+d)$$
$$+ 8bd^2(2b^2+3d^2)(24bd^4 + (31b^3+24)d^2$$
$$+ 2b^2(5b^3 - 7))z^2)\omega^3b$$
$$- 4(9(b-d)^2(b^2+4d^2)(3b^2+4d^2)$$
$$(2dt(dt+1)+1)(b+d)^2 - 12(b-d)d$$
$$(48bd^6 + 8(10b^3+9)d^4 + b^2(41b^3+16)d^2$$
$$+ 6b^4(b^3 - 3))(2dt+1)z(b+d)$$
$$+ 8d^2(12bd^4 + (11b^3 + 30)d^2 + 2b^2(b^3 - 5))$$
$$\times (12bd^4 + (17b^3 + 6)d^2 + 6b^2(b^3 - 1))z^2)\omega b$$
$$+ 64(9(b-d)^2(2dt(dt+1)+1)(b+d)^2$$
$$+ 8b^2d^2(2b^2+3d^2)^2z^2 - 12d(2b^5 + d^2b^3$$
$$- 3d^4b)(2dt+1)z)\omega^6 + 16(9(b-d)^2(15b^2$$
$$+ 8d^2)(2dt(dt+1)+1)(b+d)^2 - 12(b-d)d$$
$$(24bd^4 + (61b^3 + 6)d^2 + 6b^2(5b^3 - 1))$$
$$(2dt+1)z(b+d) + 8bd^2(2b^2+3d^2)(24bd^4$$
$$+ (61b^3+12)d^2 + 6b^2(5b^3 - 2))z^2)\omega^4$$
$$+ 4(9(b-d)^2(15b^4 + 48d^2b^2$$
$$+ 16d^4)(2dt(dt+1)+1)(b+d)^2$$
$$- 12(b-d)d(48bd^6 + 8(22b^3+3)d^4 +$$
$$3b^2(47b^3 + 28)d^2$$
$$+ 6b^4(5b^3 - 8))(2dt+1)z(b+d)$$
$$+ 8d^2(144b^2d^8 + 48b(13b^3+3)d^6$$
$$+ (775b^6 + 600b^3 + 36)d^4$$
$$+ 12b^2(31b^6 + 4b^3 - 6)d^2$$
$$+ 12b^4(5b^6 - 16b^3 + 3))z^2)\omega^2,$$

$$\Upsilon_3 = \mathrm{i}(z(-b^2 + ((b^4 - 12b^2d^2 + 6d^4)$$
$$\times((b-2\omega)((b-2\omega)^2 + 4d^2) + 4))/$$
$$(6(b-d)(b+d)(b-2\omega)((b-2\omega)^2 + 4d^2))$$
$$- 4/(b-2\omega) + 2d^2) + bt).$$

4 Conclusions

In this article, we have shown that the first-order breather solution of System (1.1) can be converted into several types of novel solitons including the W-shaped soliton (multi-peak), M-shaped soliton, periodic wave and antidark soliton. The transition condition (2.3), depending on the parameters m, n, ω, τ and b, has been analytically presented. Additionally, we have exhibited that the first-order RW solution of System (1.1) can be converted into the W-shaped soliton with single peak and two valleys when the ω, τ, and b satisfy the condition (2.3). It will be interesting to study the interactions among different kinds of nonlinear waves. We will give the details in another paper.

References

1. Agrawal, G.P.: Nonlinear Fiber Optics, 5th edn. Academic Press, London (2012)
2. Hasegawa, A., Tappert, F.D.: Transmission of stationary nonlinear optical pulses in dispersive dielectric fibers. I. Anomalous dispersion. Appl. Phys. Lett. **23**, 142 (1973)
3. Porsezian, K., Nakkeeran, K.: Optical soliton propagation in an erbium doped nonlinear light guide with higher order dispersion. Phys. Rev. Lett. **74**, 2941 (1995)
4. McCall, S.L., Hahn, E.L.: Self-induced transparency by pulsed coherent light. Phys. Rev. Lett. **18**, 908 (1967)
5. Lamb Jr., G.L.: Elements of Soliton Theory. Wiley, New York (1980)
6. Doktorov, E.V., Vlasov, R.A.: Optical solitons in media with resonant and non-resonant self-focusing nonlinearities. J. Mod. Opt. **30**, 223 (1983)
7. Maimistov, A.I., Manykin, E.A.: Propagation of ultrashort optical pulses in resonant nonlinear light guides. Sov. Phys. JETP **58**, 685 (1983)
8. Nakazawa, M., Yamada, E., Kubota, H.: Coexistence of self-induced transparency soliton and nonlinear Schrödinger soliton. Phys. Rev. Lett. **66**, 2625 (1991)

9. Porsezian, K., Mahalingam, A., Sundaram, P.S.: Solitons in the system of coupled Hirota–Maxwell–Bloch equations. Chaos Solitons Fractals **11**, 1261 (2000)

10. Nakkeeran, K.: Optical solitons in erbium doped fibers with higher order effects. Phys. Lett. A **275**, 415 (2000)

11. Yang, B., Zhang, W.G., Zhang, H.Q., Pei, S.B.: Generalized Darboux transformation and rogue wave solutions for the higher-order dispersive nonlinear Schrödinger equation. Phys. Scr. **88**, 065004 (2013)

12. Ankiewicz, A., Wang, Y., Wabnitz, S., Akhmediev, N.: Extended nonlinear Schrödinger equation with higher-order odd and even terms and its rogue wave solutions. Phys. Rev. E **89**, 012907 (2014)

13. Ankiewicz, A., Akhmediev, N.: Higher-order integrable evolution equation and its soliton solutions. Phys. Lett. A **378**, 358 (2014)

14. Davydova, T.A., Zaliznyak, Y.A.: Schrödinger ordinary solitons and chirped solitons: fourth-order dispersive effects and cubic-quintic nonlinearity. Phys. D **156**, 260 (2001)

15. Li, L.J., Wu, Z.W., Wang, L.H., He, J.S.: High-order rogue waves for the Hirota equation. Ann. Phys. **334**, 198 (2013)

16. Guo, R., Hao, H.Q.: Breathers and localized solitons for the Hirota–Maxwell–Bloch system on constant backgrounds in erbium doped fibers. Ann. Phys. **344**, 10 (2014)

17. Guo, R., Hao, H.Q.: Propagation properties of soliton solutions under the influence of higher order effects in erbium doped fibers. Commun. Nonlinear Sci. Numer. Simul. **19**, 3529 (2014)

18. Guo, R., Hao, H.Q., Gu, X.S.: Modulation instability, breathers, and bound solitons in an erbium-doped fiber system with higher-order effects. Abstr. Appl. Anal. **2014**, 185654 (2014)

19. Zhang, Y., Li, C.Z., He, J.S.: Rogue waves in a resonant erbium-doped fiber system with higher-order effects. arXiv:1505.02237

20. Wang, Q.M., Gao, Y.T., Su, C.Q., Zuo, D.W.: Solitons, breathers and rogue waves for a higher-order nonlinear Schrödinger Maxwell–Bloch system in an erbium-doped fiber system. Phys. Scr. **90**, 105202 (2015)

21. Su, C.Q., Gao, Y.T., Xue, L., Yu, X.: Solitons and rogue waves for a higher-order nonlinear Schrödinger–Maxwell–Bloch system in an erbium-doped fiber. Z. Naturforsch. A **70**, 935 (2015)

22. Zuo, D.W., Gao, Y.T., Feng, Y.J., Xue, L.: Rogue-wave interaction for a higher-order nonlinear Schrödinger–Maxwell–Bloch system in the optical-fiber communication. Nonlinear Dyn. **78**, 2309 (2014)

23. Li, J.T., Han, J.Z., Du, Y.D., Dai, C.Q.: Controllable behaviors of Peregrine soliton with two peaks in a birefringent fiber with higher-order effects. Nonlinear Dyn. **82**, 1393 (2015)

24. Xie, X.Y., Tian, B., Sun, W.R., Sun, Y.: Rogue-wave solutions for the Kundu–Eckhaus equation with variable coefficients in an optical fiber. Nonlinear Dyn. **81**, 1349 (2015)

25. Yang, Y.Q., Wang, X., Yan, Z.Y.: Optical temporal rogue waves in the generalized inhomogeneous nonlinear Schrödinger equation with varying higher-order even and odd terms. Nonlinear Dyn. **81**, 833 (2015)

26. Sun, W.R., Tian, B., Zhen, H.L., Sun, Y.: Breathers and rogue waves of the fifth-order nonlinear Schrödinger equation in the Heisenberg ferromagnetic spin chain. Nonlinear Dyn. **81**, 725 (2015)

27. Meng, G.Q., Qin, J.L., Yu, G.L.: Breather and rogue wave solutions for a nonlinear Schrödinger-type system in plasmas. Nonlinear Dyn. **81**, 739 (2015)

28. Chen, H.Y., Zhu, H.P.: Controllable behaviors of spatiotemporal breathers in a generalized variable-coefficient nonlinear Schrödinger model from arterial mechanics and optical fibers. Nonlinear Dyn. **81**, 141 (2015)

29. Guo, R., Liu, Y.F., Hao, H.Q., Qi, F.H.: Coherently coupled solitons, breathers and rogue waves for polarized optical waves in an isotropic medium. Nonlinear Dyn. **80**, 1221 (2015)

30. Yan, Z.Y.: Two-dimensional vector rogue wave excitations and controlling parameters in the two-component Gross–Pitaevskii equations with varying potentials. Nonlinear Dyn. **79**, 2515 (2015)

31. Zhu, H.P.: Spatiotemporal solitons on cnoidal wave backgrounds in three media with different distributed transverse diffraction and dispersion. Nonlinear Dyn. **76**, 1651 (2014)

32. Yu, F.J.: Matter rogue waves and management by external potentials for coupled Gross–Pitaevskii equation. Nonlinear Dyn. **80**, 685 (2015)

33. Guo, R., Hao, H.Q., Zhang, L.L.: Dynamic behaviors of the breather solutions for the AB system in fluid mechanics. Nonlinear Dyn. **74**, 701 (2013)

34. Dai, C.Q., Wang, Y.Y.: Controllable combined Peregrine soliton and Kuznetsov–Ma soliton in PT-symmetric nonlinear couplers with gain and loss. Nonlinear Dyn. **80**, 715 (2015)

35. Dai, C.Q., Wang, X.G., Zhou, G.Q.: Stable light-bullet solutions in the harmonic and parity-time-symmetric potentials. Phys. Rev. A **89**, 013834 (2014)

36. Dai, C.Q., Wang, Y.Y.: Superposed Akhmediev breather of the (3+1)-dimensional generalized nonlinear Schrödinger equation with external potentials. Ann. Phys. **341**, 142 (2014)

37. Dai, C.Q., Wang, Y.Y., Zhang, X.F.: Controllable Akhmediev breather and Kuznetsov–Ma soliton trains in PT-symmetric coupled waveguides. Opt. Express **22**, 29862 (2014)

38. Kedziora, D.J., Ankiewicz, A., Akhmediev, N.: Second-order nonlinear Schrödinger equation breather solutions in the degenerate and rogue wave limits. Phys. Rev. E **85**, 066601 (2012)

39. Ren, Y., Yang, Z.Y., Liu, C., Yang, W.L.: Different types of nonlinear localized and periodic waves in an erbium-doped fiber system. Phys. Lett. A **379**, 45 (2015)

40. Chowdury, A., Ankiewicz, A., Akhmediev, N.: Moving breathers and breather-to-soliton conversions for the Hirota equation. Proc. R. Soc. A **471**, 20150130 (2015)

41. Chowdury, A., Kedziora, D.J., Ankiewicz, A., Akhmediev, N.: Breather-to-soliton conversions described by the quintic equation of the nonlinear Schrödinger hierarchy. Phys. Rev. E **91**, 032928 (2015)

42. Liu, C., Yang, Z.Y., Zhao, L.C., Yang, W.L.: Transition, coexistence, and interaction of vector localized waves arising from higher-order effects. Ann. Phys. **362**, 130 (2015)

43. Liu, C., Yang, Z.Y., Zhao, L.C., Yang, W.L.: State transition induced by higher-order effects and background frequency. Phys. Rev. E **91**, 022904 (2015)

44. Barashenkov, I.V., Smirnov, Y.S.: Existence and stability chart for the ac-driven, damped nonlinear Schrödinger solitons. Phys. Rev. E **54**, 5707 (1996)

45. Barashenkov, I.V., Zemlyanaya, E.V.: Travelling solitons in the externally driven nonlinear Schrödinger equation. J. Phys. A Math. Theor. **44**, 465211 (2011)

46. Kivshar, Y.S.: Nonlinear dynamics near the zero-dispersion point in optical fibers. Phys. Rev. A **43**, 1677 (1991)

47. Kivshar, Y.S., Afanasjev, V.V.: Dark optical solitons with reverse-sign amplitude. Phys. Rev. A **44**, 1446(R) (1991)

48. He, J.S., Xu, S.W., Ruderman, M.S., Erdelyi, R.: State transition induced by self-steepening and self phase-modulation. Chin. Phys. Lett. **31**, 010502 (2014)

49. He, J.S., Xu, S.W., Cheng, Y.: The rational solutions of the mixed nonlinear Schrödinger equation. AIP Adv. **5**, 017105 (2015)